Aptamer Displacement Identifies Alternative Small-Molecule Target Sites that Escape Viral Resistance

Satoko Yamazaki,[1,5,6] Lu Tan,[2,5,7] Günter Mayer,[1,6] Jörg S. Hartig,[1,6] Jin-Na Song,[1,6] Sandra Reuter,[3,8] Tobias Restle,[4,9] Sandra D. Laufer,[4,9] Dina Grohmann,[4,9] Hans-Georg Kräusslich,[3,8] Jürgen Bajorath,[2,7,*] and Michael Famulok[1,6,*]

[1] LIMES Program Unit Chemical Biology & Medicinal Chemistry, c/o Kekulé Institute for Organic Chemistry & Biochemistry, University of Bonn, Gerhard-Domagk-Strasse 1, D-53121 Bonn, Germany
[2] Department of Life Science Informatics, B-IT, University of Bonn, Dahlmannstrasse 2, D-53113 Bonn, Germany
[3] Department of Virology, University of Heidelberg, Im Neuenheimer Feld 324, D-69120 Heidelberg, Germany
[4] Institute of Molecular Medicine, University of Lübeck, Ratzeburger Allee 160, D-23538 Lübeck, Germany
[5] These authors contributed equally to this work.
[6] Lab address: http://www.chembiol.uni-bonn.de/
[7] Lab address: http://www.b-it-center.de/Wob/en/view/class211_id231.html
[8] Lab address: http://www.klinikum.uni-heidelberg.de/index.php?id=4722&L=en
[9] Lab address: http://www.molmed.uni-luebeck.de/T.%20Restle/Restle.html
*Correspondence: bajorath@bit.uni-bonn.de (J.B.), m.famulok@uni-bonn.de (M.F.)
DOI 10.1016/j.chembiol.2007.06.003

SUMMARY

Aptamers targeting reverse transcriptase (RT) from HIV-1 inhibit viral replication in vitro, presumably by competing with binding of the primer/template complex. This site is not targeted by the currently available small-molecule anti-HIV-1 RT inhibitors. We have identified SY-3E4, a small-molecule inhibitor of HIV-1 RT, by applying a screening assay that utilizes a reporter-ribozyme regulated by the anti-HIV-1 RT aptamer. SY-3E4 displaces the aptamer from the protein, selectively inhibits DNA-dependent, but not RNA-dependent, polymerase activity, and inhibits the replication of both the wild-type virus and a multidrug-resistant strain. Analysis of available structural data of HIV-1 and HIV-2 RTs rationalizes many of the observed characteristics of the inhibitory profiles of SY-3E4 and the aptamer and suggests a previously not considered region in these RTs as a target for antiviral therapy. Our study reveals unexplored ways for rapidly identifying alternative small-molecule target sites in proteins and illustrates strategies for overcoming resistance-conferring mutations with small molecules.

INTRODUCTION

It is estimated that "chemical space"—the total possible number of small carbon-based drug-like compounds with molecular masses of up to 500 Da—might be 10^{60} or greater [1, 2]. In contrast, fewer than 30 million mole-cules are registered in Chemical Abstracts, and only a subset of these has biological relevance [3]. This raises the question of how one might effectively explore chemical space to identify molecules of biological or medicinal interest. Toward this goal, we have developed approaches that combine Darwinian evolution of biomolecules with small-molecule screening [4–6]. Biomolecules continuously adapt their functional properties to external conditions by mechanisms through which superior features emerge from a combination of genetic alterations and survival of selective pressures. These features are passed on to subsequent generations. The same principles can be applied in vitro to select for aptamers from libraries with a molecular diversity of up to 10^{16} different structured nucleic acid sequences, the highest degree of diversity currently amenable to screening. Aptamers can serve as specific inhibitors of virtually any given protein target, but the main obstacle to achieving broadly applicable inhibition of target proteins in cells, tissues, and whole organisms by aptamer technology is delivery. In addition, these approaches have limited, if any, clinical use. For such purposes, drug-quality small molecules are highly advantageous compared to any nucleic acid- or biopolymer-based inhibitor, both as research tools and as starting points for drug development. Therefore, we have developed strategies that enable the conversion of an aptamer/protein complex into a small organic inhibitor by screening small-molecule libraries for compounds that displace the aptamer from its target and adopt its inhibitory activity [5, 6]. This allows for small molecules with similar inhibitory activities as the parent aptamer to be searched for directly. Here, we have used this approach to explore the possibility of identifying novel classes of inhibitors targeting reverse transcriptase of HIV-1 (HIV-1 RT) at different sites than the currently available anti-HIV-1 RT inhibitors. Based on a structurally well-characterized RNA

aptamer that inhibits HIV-1 RT with high specificity [7, 8], we identified such a small-molecule inhibitor and rationalized its binding and inhibitory characteristics by using crystallographic and mutant data. Our results show that novel types of active small molecules can be identified with the aid of reporter ribozyme probes against established protein targets. The newly identified inhibitor circumvents some of the current limitations associated with small-molecule HIV-RT inhibitors caused by drug-resistant mutations and might provide a previously unexplored opportunity for antiviral therapy.

RESULTS

Converting the Anti-HIV-1 RT Aptamer into a Small Molecule

To convert the inhibitory profile of the anti-HIV-1 RT aptamer into a drug-like inhibitor, we established a screening assay based on a rationally designed allosteric hammerhead ribozyme that is able to detect HIV-1 RT with high selectivity [7]. The ribozyme is regulated by a variant of a small aptamer that forms a pseudoknot structure in the presence of the protein [8], rendering the ribozyme inactive, but folds into a stem-loop structure with an internal bulge in its absence [7], resulting in ribozyme activation (Figure 1A; see Figure S1 in the Supplemental Data available with this article online). This allosteric ribozyme exhibits extraordinary selectivity for HIV-1 RT, as it cannot be regulated by RTs from even closely related viruses such as RT from HIV-2. In its active form, the ribozyme cleaves an RNA substrate labeled with a fluorophor on its 5′ end and a quencher molecule, tetramethylamino rhodamine, on its 3′ end. Due to fluorescence resonance energy transfer (FRET), fluorescence of the uncleaved substrate is quenched [5], whereas cleavage results in dissociation of the substrate fragments and fluorescence dequenching. The general principles of allosteric ribozymes have been utilized in various sensors and reporter applications [9–13].

By screening a diverse library of synthetic chemicals with this assay, we identified a series of compounds as initial hits that were able to reactivate the ribozyme, presumably by displacing the aptamer domain from the bound RT (Figure S1). Based on their behavior in the reporter ribozyme assay, the most promising compounds, SY-3E4 and SY-2E10, both representing substituted N,N′-diphenylurea derivatives, were selected for synthesis and further studies (Figure 1B; Supplemental Data and Figure S2).

To confirm that SY-3E4 displaces the aptamer from the protein rather than activating the reporter ribozyme by a different mechanism, we performed an assay in which the complex of HIV-1 RT and the isolated 5′-^{32}P-labeled aptamer was immobilized on nitrocellulose in the presence of increasing concentrations of the compound. As a control, the same experiment was done with nevirapine, a small molecule that binds HIV-1 RT in a way that does not interfere with aptamer binding (Figure 1C). As evident, the amount of aptamer/protein complex is reduced at SY-3E4 concentrations above 50 μM, whereas high concen-

trations of nevirapine had no influence on complex stability. These data show that the screening assay identified SY-3E4 by a mechanism by which the compound interfered with the formation of the aptamer/protein complex.

RT Inhibition Is Template Dependent

We analyzed the inhibitory potential of these compounds in a primer-elongation assay (Figure 1D) with radiolabeled primers, dNTPs, either RNA or DNA templates, and either reverse transcriptase or DNA polymerase from various organisms. Table 1 summarizes the IC$_{50}$ values obtained for the two molecules in both RNA- and DNA-templated primer-elongation assays (also see Figure S5).

Impressively, both compounds showed marked differences in their inhibitory potential depending on whether RNA or DNA was used as a template in the primer-elongation assay. With HIV-1 RT, SY-3E4 exhibited the lowest IC$_{50}$ values of 2.1 μM, but only in the DNA-dependent (DD) primer elongations. In the RNA-dependent (RD) assay, the inhibitory potential of this compound was reduced almost 70-fold. In contrast, while SY-2E10 also inhibited HIV-1 RT with an IC$_{50}$ value of 3.7 μM, its discrimination between DD and RD assays was less than 3-fold. A very similar inhibitory profile was also observed when using HIV-2 RT as a target. SY-3E4 inhibits HIV-2 RT with an IC$_{50}$ value of 9.4 μM in DD polymerization, and it discriminates between DD and RD polymerizations 17-fold. SY-2E10 showed an IC$_{50}$ value of 5.1 μM, with 2-fold discrimination between DD and RD polymerizations.

We also performed control reactions with other reverse transcriptases and DNA polymerases (Table 1). Inhibition of RT from avian myoblastoma virus (AMV) by SY-3E4 was marginal in both DD and RD primer extensions (∼64 μM), whereas SY-2E10 showed an IC$_{50}$ value of 7.2 μM for DD polymerizations, with <4.5-fold discrimination to the disadvantage of the RD reaction. SY-3E4 also exhibited a moderate IC$_{50}$ value of 21 μM when Moloney murine leukemia virus (MMLV) RT was used in the DD reaction, with 2-fold discrimination to the disadvantage of the RD polymerization. In contrast, Klenow fragment DNA polymerase (KF) was insignificantly inhibited by SY-3E4 and was moderately inhibited by SY-2E10. Polymerase β (Polβ) was moderately inhibited by SY-3E4, whereas the IC$_{50}$ value of SY-2E10 was 12.3 μM (Table 1).

Taken together, these data show that, particularly, SY-3E4 specifically inhibits the DNA-dependent, but not RNA-dependent, primer-elongation activity of reverse transcriptases from HIV-1 and HIV-2. Other RTs or DNA polymerases are either not targeted or only marginally blocked by this inhibitor. The selectivity of SY-2E10 for HIV RTs and also for the used template was much less pronounced. This inhibitor also showed weak inhibition of RTs and DNA polymerases from other organisms.

SY-3E4 Inhibits HIV-1 Replication for Wild-Type and a Multidrug-Resistant Strain

SY-3E4, the identified compound that showed the best specificity and IC$_{50}$ values for HIV-1 and HIV-2 RTs, was then assayed for its ability to reduce HIV-1 replication in
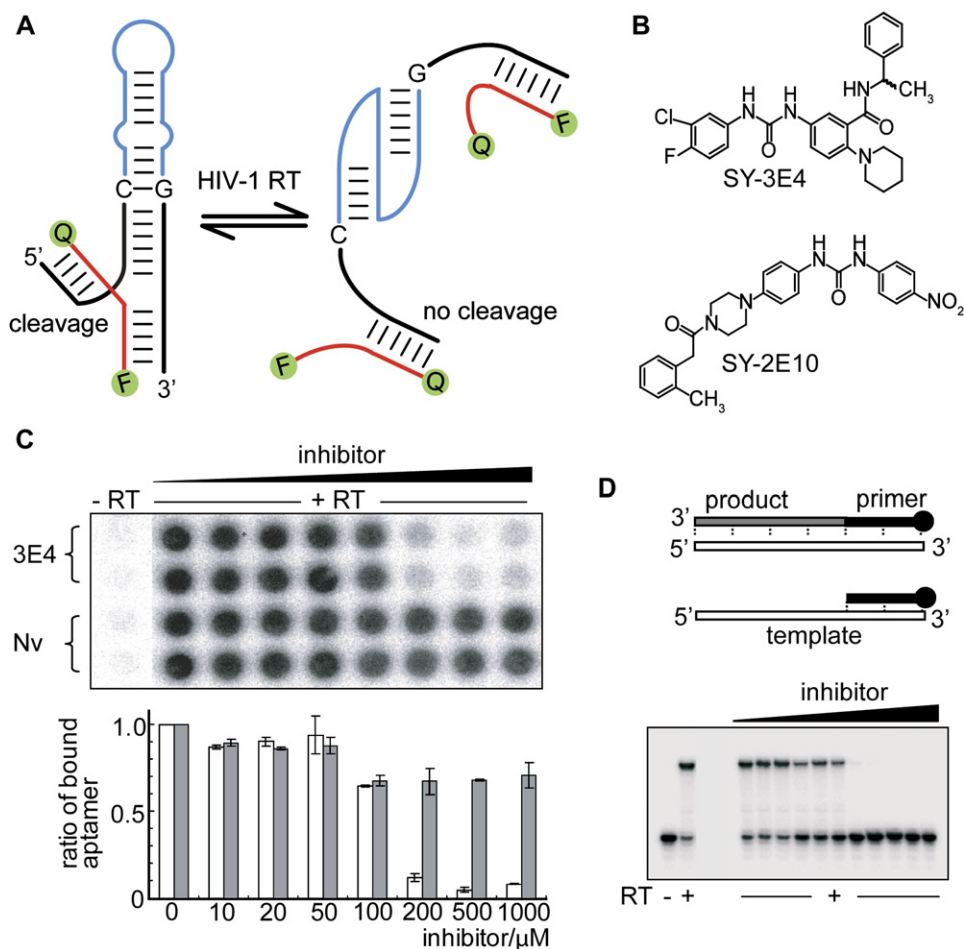
Figure 1. Structure and Function of Identified Inhibitors

(A) Schematic for the HIV-1 RT-responsive hammerhead ribozyme used in the screening assay. In the presence of HIV-1 RT, the aptamer sequence (blue) adopts a pseudoknot structure, disrupting the formation of stem II (left). The additional GC pair was introduced to enforce the formation of the stem-loop structure (left) in the absence of HIV-1 RT (also see Figure S1C for sequences).

(B) Chemical structures of the obtained compounds, SY-3E4 and SY-2E10.

(C) SY-3E4 displaces the isolated aptamer complexed to HIV-1 RT. Upper panel: duplicate dot-blot analysis of 5'-^{32}P-labeled aptamer/RT complex retained on nitrocellulose filters at increasing concentrations of SY-3E4 and nevirapine (Nv). Lower panel: quantification of the dot-blot analysis by PhosphorImaging. Error bars represent standard deviations for duplicates.

(D) Representative example showing the inhibition of DNA polymerase activity of HIV-1 RT by small-molecule inhibitors. In the presence of HIV-1 RT, the 5'-end-labeled primer is extended by employing either a DNA or RNA template (top panel). The control lane in the absence of HIV-1 RT (−) shows the primer position. Polymerization reactions were inhibited by the addition of increasing concentrations of inhibitors (bottom panel, right lanes). The inhibitor concentrations ranged from 0.5 μM to 50 μM.

tissue culture cells. At concentrations between 10 and 100 μM, no cytotoxicity was observed for SY-3E4 and SY-2E10 (data not shown). We then measured the inhibitory potential of all compounds in a self-inactivating HIV vector system [14] (Figure S3A). SY-3E4 showed substantial reduction of reporter gene expression in a concentration-dependent manner. However, with SY-2E10, the same level of luciferase activity as in the negative control experiments was observed, indicating that SY-2E10 has no effect in this reporter gene assay (Figure S3B). At present, we do not have an explanation for the lack of in vivo inhibitory activity of SY-2E10. Possible reasons for this observation may be poor uptake of this compound by the cells or a short half-life under these conditions. Half-maximal

reduction of luciferase expression by SY-3E4 was obtained at 5.3 μM, a value that is in the same order of magnitude as the IC$_{50}$ values measured in the primer-elongation assays in vitro.

Encouraged by these results, we next investigated the effect of SY-3E4 on the expression of a luciferase reporter gene under the control of the HIV-1 long terminal repeat (LTR) promoter [15] in TZM cells infected with the wild-type HIV-1 strain NL4-3. As shown in Figure 2A, luciferase gene expression was dramatically reduced in the presence of SY-3E4 in a concentration-dependent fashion, reaching complete inhibition at 30 μM concentrations, and a half-maximal reduction at less than 20 μM. These data are in accordance with the results shown in

Table 1. IC$_{50}$ Values of SY-3E4 and SY-2E10 for Different DNA Polymerases and Reverse Transcriptases

RT Strain	Template	SY-3E4 IC$_{50}$ (μM)[a]	SY-2E10
HIV-1	DD	2.1 ± 0.6	3.7 ± 0.1
	RD	145 ± 5.1	10.8 ± 0.9
HIV-2	DD	9.4 ± 0.2	5.1 ± 0.1
	RD	160 ± 19.1	10.3 ± 0.9
AMV	DD	64.1 ± 2.6	7.3 ± 0.2
	RD	63.7 ± 7.8	32.0 ± 4.8
MMLV	DD	21.2 ± 0.9	12.2 ± 0.1
	RD	42.5 ± 1.2	16.4 ± 0.4
KF$^-$	DD	99.7 ± 3.3	22.8 ± 0.5
Polβ	DD	30.4 ± 0.8	12.3 ± 0.1

DD, DNA-dependent DNA polymerase activity; RD, RNA-dependent DNA polymerase activity.
[a] The mean values ± standard deviations obtained from two independent experiments are shown.

Figure S3B. In contrast, SY-2E10 was again inactive in this assay, as expected from the results with the self-inactivating HIV vector system. In a second experiment, we investigated the effect of the selected compounds on the number of HIV-1-infected cells. To this end, we grew HIV-1 by coculturing an infected and uninfected T cell line in the presence or absence of drug and determined the titer again by using TZM cells, which express β-galactosidase under the control of the HIV-1 LTR promoter, thus enabling colorimetric detection and enumeration of the HIV-1-infected cells. The infectivity of intact HIV-1 NL4-3 virus was arbitrarily set at 100%. In accordance with the previous experiments, SY-3E4 reduced the number of infected cells considerably, in contrast to SY-2E10. Complete loss of infectivity was observed with 30 μM SY-3E4, with an IC$_{50}$ value of 15 μM (Figure 2B).

To investigate the effect of SY-3E4 on the replication of a multidrug-resistant strain of HIV-1, we performed an inhibition experiment with the virus TN6-P5-5, carrying the protease- and RT genes from a highly resistant, patient-derived HIV-1 in the genetic background of the NL4-3 strain (see Supplemental Data for mutations in RT of TN6-P5-5). This strain had been shown to be resistant against a series of NNRTI and NRTI drugs (e.g., AZT, Tenofovir, and Efavirenz), and its resistance profile was confirmed in our experiments by using a direct comparison with NL4-3 (Figure 2C, middle panels). Importantly, however, SY-3E4 showed essentially no difference in its ability to inhibit wild-type HIV-1 and the multidrug-resistant strain (Figure 2C, left panel), indicating that it is not affected by the resistance-conferring mutations in TN6-P5-5. As before, SY-2E10 had no effect on NL4-3, nor on the mutant strain.

SY-3E4 Competes with Primer/Template Complex Binding to HIV-1 RT

We have previously shown that the addition of a DNA primer/template complex [16] results in competitive displacement of the HIV-1 RT reporter ribozyme from the enzyme, leading to reactivation of the ribozyme cleavage reaction [7]. Therefore, to further elucidate the possible mechanism of action of SY-3E4, we investigated whether the inhibitor would also be able to compete with primer/template complexes bound to HIV-1 RT. We performed an electrophoretic mobility shift assay (EMSA) in which the amounts of primer/template/HIV-1 RT complexes obtained at various concentrations of SY-3E4 were quantified. As shown in Figure 2D, SY-3E4 was able to compete with the primer/template complex for HIV-1 RT binding, whereas nevirapine, an NNRTI that binds outside the primer/template site, was inactive. However, competition by SY-3E4 was efficient only at concentrations above 100 μM. Furthermore, both the DNA primer/DNA and RNA template complexes were competed. Competition of the DNA primer/RNA template complex was even slightly more efficient, with approximately 200 μM half-maximal concentration of competition, than the DNA primer/DNA template complex (~500 μM). Thus, the half-maximal concentration of competition measured for the DNA primer/RNA template complex displacement matches well with the IC$_{50}$ value obtained for the corresponding HIV-1 RT inhibition reaction (Table 1). The same is true when the aptamer was used as a competitor (Figure 2D, left panel, lanes 10 and 18; right panel, lane A), indicating that, in these cases, the inhibitory mechanism is largely determined by competition with the primer/template complex. In contrast, the half-maximal concentration of competition
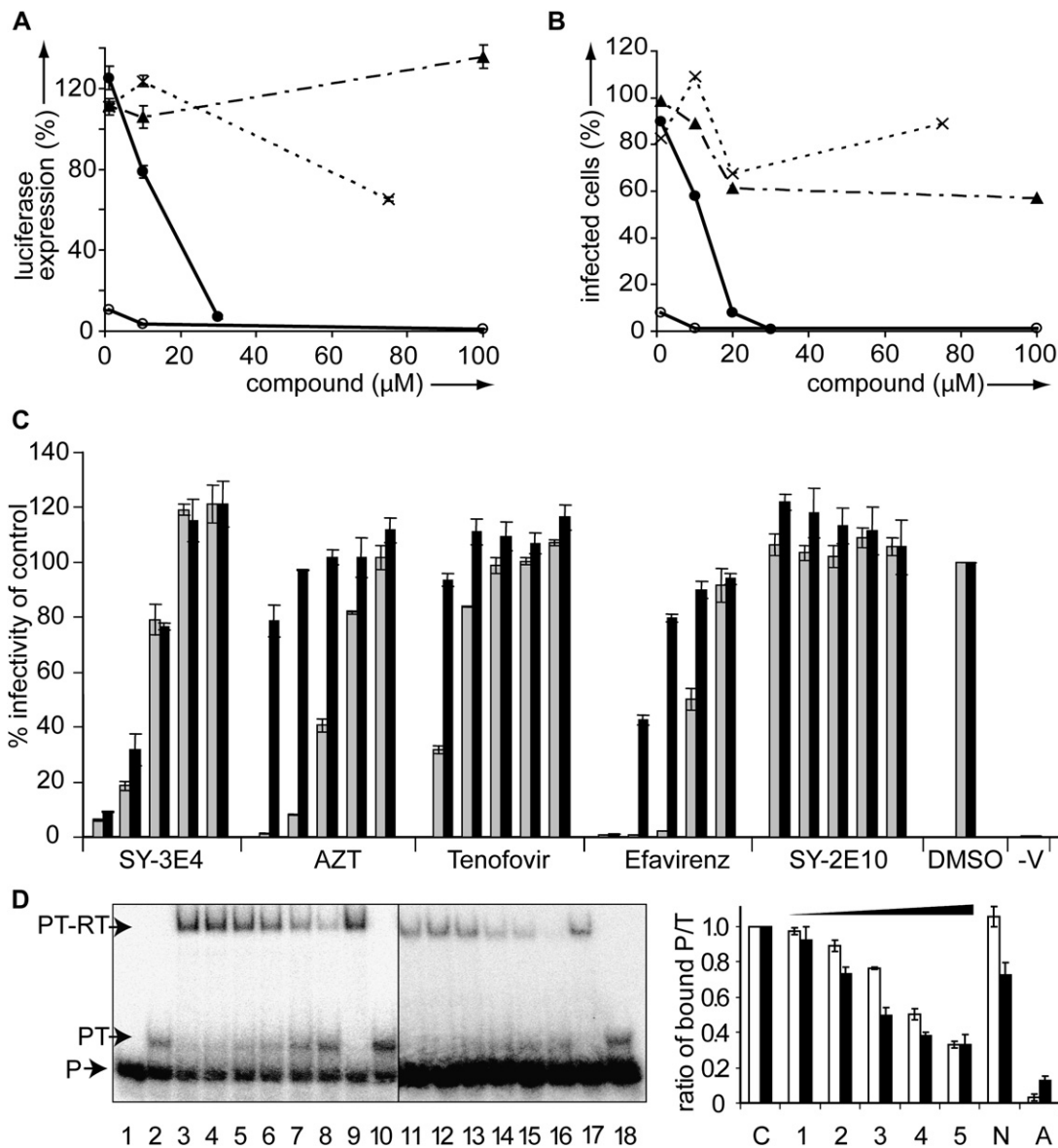
Figure 2. Inhibition of HIV-1 Replication by Small-Molecule Inhibitors

(A) HIV-1 replication was investigated in TZM reporter cells infected with HIV-1 strain NL4-3 wild-type virus in the presence of 3E4 (filled circles) or 2E10 (filled triangles), the negative control (multiplication signs), or AZT as the positive control (open circles). The mean percentage of luciferase marker gene expression compared with untreated control cells from at least two replicate infections is shown.

(B) TZM cells were infected with HIV-1 strain NL4-3, and numbers of infected cells were counted after staining with β-galactosidase substrate after 48 hr. Values are expressed as the percentage of the number of infected cells without inhibitors, which was set to 100%. The mean of duplicates is shown. 3E4, filled circles; 2E10, filled triangles; negative control, multiplication signs; and AZT, open circles.

(C) Comparison of inhibition of the wild-type strain NL4-3 (gray bars) and the multidrug-resistant mutant TN6-P5-5 (black bars) with various inhibitors. Inhibitor concentrations were matched according to the different IC_{50} values (from right to left: SY-2E10: 0.1, 1, 5, 10, 20 μM; Efavirenz: 0.1, 1.0, 10, 100, 1000 nM; Tenofovir: 0.001, 0.01, 0.1, 1, 10 μM; AZT: 0.001, 0.01, 0.1, 1, 10 μM; SY-3E4: 0.1, 1, 5, 10, 20 μM). The y axis shows the percent infectivity of control, where the control is the parallel infection with DMSO-treated virus, which was arbitrarily set at 100%. Error bars represent standard deviations for triplicates.

(D) SY-3E4 interferes with primer/template binding to HIV-1 RT at high concentrations. Left panel: gel shift of radiolabeled primer (P), complexed to the DNA template (lanes 2–10) or RNA template (lanes 11–18), respectively, in the absence (PT) and presence of HIV-1 RT (PT-RT complex). Lanes 3–10: complex of DNA template, primer, and HIV-1 RT in the presence of 0 (lane 3), 50 μM (lane 4), 100 μM (lane 5), 200 μM (lane 6), 500 μM (lane 7), 1 mM (lane 8) SY-3E4; 1 mM nevirapine (lane 9); and 0.5 nM aptamer (lane 10). Lanes 11–18: complex of RNA template, primer, and HIV-1 RT in the presence of 0 (lane 11), 50 μM (lane 12), 100 μM (lane 13), 200 μM (lane 14), 500 μM (lane 15), 1 mM (lane 16) SY-3E4; 1 mM nevirapine (lane 17); and 0.5 nM aptamer (lane 18). Right panel: ratio of primer/template complex bound to HIV-1 RT quantified from the gel-shift experiments. White bars, primer-DNA template; black bars, primer-RNA template. C: DMSO negative control, 50 μM (lane 1), 100 μM (lane 2), 200 μM (lane 3), 500 μM (lane 4), 1 mM (lane 5) SY-3E4; 1 mM nevirapine (N); and 0.5 nM aptamer (A). Error bars represent standard deviations for duplicates.

seen for the DNA primer/DNA template complex was ~200-fold higher than the IC$_{50}$ value, which means that the mechanism of inhibition by SY-3E4 cannot solely be explained on the basis of competition with the primer/template complex.

Figure S4 shows the structure of HIV-1 RT in a trapped complex with a DNA primer/RNA template hybrid [17] and summarizes known features of the polymerization mechanism. On the basis of currently available data, it is not possible to explain the inhibitory preference of SY-3E4 for the DD reaction in molecular detail. However, the RNA in the RNA/DNA complex is only partly present during catalysis, the partial complex is much more transient than the DNA/DNA complex, and the RNA-dependent polymerization efficiency is higher (Figure S4). These features suggest that the RNA/DNA complex might provide a more difficult target for small-molecule interference and competition than the more stable and catalytically less efficient DNA/DNA complex.

Rationalization of Inhibitor Characteristics and Target Sites

Taken together, SY-3E4 exhibits the following characteristics: (1) the inhibitor displaces the anti-HIV-1 RT aptamer bound to its target; (2) it inhibits RTs from both HIV-1 and HIV-2, whereas the aptamer inhibited only HIV-1 RT, and (3) it predominantly inhibits DNA-dependent polymerization; (4) SY-3E4 inhibition is not affected by the common NRTI- and NNRTI-resistant mutations; and (5) SY-3E4 competition of primer/template complexes occurs only at high concentrations and does not discriminate between DNA and RNA templates.

Based on the analysis of available crystallographic structures and mutant data, characteristic features of the aptamer and SY-3E4 inhibitor profiles can be well rationalized. Figure 3A shows a view of a high-resolution structure of HIV-1 RT [18]. The representation highlights the fingers, palm, thumb, and RNase H domains in the p66 subunit of the enzyme. Furthermore, it shows the locations of the NRTI drug-binding site, indicated by bound dNTP [19], and the NNRTI-binding site with bound nevirapine [18]. For residue mapping analysis, we have transferred the bound aptamer from its low-resolution complex with HIV-1 RT [20] to the high-resolution structure [18] after optimal superposition of protein backbone atoms. In Figure 3B, sites of natural mutations causing NRTI and NNRTI drug resistance [21] are displayed. NRTI drug-resistant mutations primarily map to the fingers domain, and NNRTI drug-resistant mutations map to the palm and thumb domains (Table S1). No drug-resistant mutations were found in the aptamer-binding region, however. Therefore, the most plausible explanation for aptamer replacement by SY-3E4 is that the inhibitor also binds to the aptamer-binding region. This is supported by the finding that SY-3E4 binding was not affected by known drug-resistant mutations, which all reside outside the aptamer-binding site.

An important difference in specificity between SY-3E4 and the aptamer is that SY-3E4 inhibits both HIV-1 and HIV-2 RT, whereas the aptamer only binds HIV-1 RT
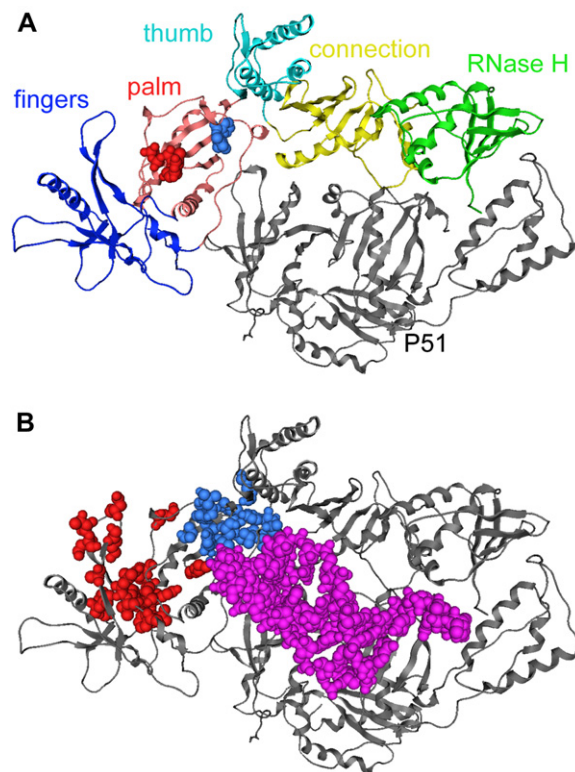

Figure 3. Structure of HIV-1 RT, Location of Drug-Resistant Mutations, and the Aptamer-Binding Site

(A) Structural overview of HIV-1 RT, a heterodimer composed of two subunits, the catalytic active p66 and the p51 subunit. In p66, the fingers (blue), palm (carnation), and thumb (cyan) domains are highlighted. The polymerase active site is located in the palm domain. The substrate analog dTTP (space-filling representation, red) binds at the same polymerase active site location as NRTI drugs. By contrast, NNRTI drugs such as nevirapine (space-filling, light blue) bind at the interface between the palm and thumb domains. Also highlighted is the RNase H (green) domain that removes RNA during reverse transcription. The domains responsible for the polymerase and endonuclease activities are linked by a connecting domain (yellow). The p51 subunit (gray) does not participate in catalytic activities.

(B) Residues that are hot spots for natural mutations causing NRTI drug resistance (red) are mainly located in the fingers domain, whereas mutated residues causing NNRTI drug resistance (light blue) are distributed over parts of the palm and thumb domains. Sites of mapped NRTI and NNRTI drug-resistant mutations are colored in red and light blue, respectively. The aptamer (magenta) extends along the nucleic acid-binding cleft and overlaps with the primer/template-binding site, but does not protrude into the palm and polymerase active site region. Mapping of mutants and the aptamer-binding site reveals that the NRTI/NNRTI drug-resistant sites and the aptamer-binding site are located in distinct regions of HIV-1 RT.

[22]. In Figure 4A, changes in surface-residue positions between HIV-1 and HIV-2 RT [23] are mapped. As can be seen, the region in HIV-2 RT that corresponds to the aptamer-binding site in HIV-1 RT contains many surface-residue replacements relative to HIV-1 RT that include aptamer contact residues. The nonconservation of residues mediating HIV-1 RT/aptamer interactions explains why the aptamer does not bind to HIV-2 RT.
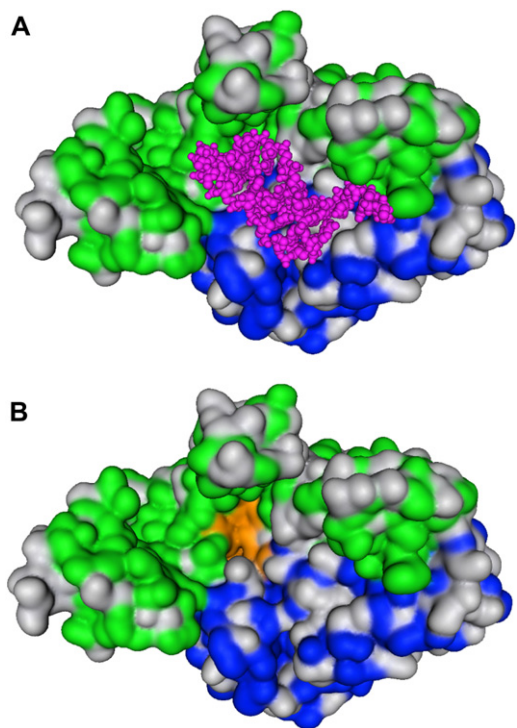
Figure 4. Mapping of HIV-RT Surface Residues

Shown is a solvent-accessible surface representation of HIV-1 RT in the same orientation as in Figure 3; the p66 and p51 subunits are colored green and blue, respectively.

(A) Surface-residue variation between HIV-1 RT and HIV-2 RT. Residue positions that are not conserved are shown in white, and the aptamer is shown in magenta. There are extensive residue changes between HIV-1 RT and HIV-2 RT involving aptamer contact residues in HIV-1 RT.

(B) Depiction of an attractive candidate site for small-molecule binding (orange), a deep pocket formed by residues conserved in HIV-1 RT and HIV-2 RT. This pocket is located within the aptamer-binding region.

However, despite substantial variation of surface residues in HIV-1 and HIV-2 RT, the aptamer-binding region contains clusters of residues that are conserved in both enzymes. A cavity highlighted in Figure 4B presents a likely site for small-molecule binding. This deep and largely hydrophobic pocket is formed by residues that are conserved in HIV-1 and HIV-2 RT. While identification of the exact SY-3E4-binding site awaits crystallographic analysis of an RT/SY-3E4 complex (or transfer NOE experiments), we can conclude that the aptamer-binding surface in HIV-1 RT contains a region that is conserved in HIV-2 RT and provides an attractive and previously unobserved target site for small molecules.

DISCUSSION

In this study, we have identified a novel small-molecule inhibitor of HIV-1 and HIV-2 RT through a displacement assay with an HIV-1 RT-specific aptamer. The data reported above show that this assay based on the RT-responsive reporter ribozymes was able to quickly and robustly identify a previously unknown, to our knowledge, inhibitor of

HIV-1 replication. SY-3E4 might serve as an interesting lead compound to find small molecules that are even more potent in reducing retrovirus replication. The finding that SY-3E4 inhibits both HIV-1 and HIV-2 RT, with moderate 4.5-fold discrimination of SY-3E4 in favor of HIV-1 RT, is interesting because the aptazyme displaced by this compound discriminates between these related enzymes quite well [7]. Analysis of surface-residue conservation in HIV-1 and HIV-2 RT explained the specificity of the aptamer. Another key finding has been that the function of SY-3E4 was not affected by known drug-resistant mutations, and this molecule may thus provide new opportunities for antiviral HIV therapy. The inhibitor characteristics of the aptamer and SY-3E4 are well in accord with available structural data, and, on the basis of our analysis, we can point at a region in HIV-1 and HIV-2 RT outside the polymerase active site and its vicinity that provides a promising target site for small molecules to interfere with the formation of the primer/template complex.

The ability of SY-3E4 to compete with primer/template complex binding to HIV-1 RT at high concentrations is consistent with the proposed presence of a small-molecule binding region outside the polymerase active site. The concentration of SY-3E4 required to inhibit the DNA-dependent polymerase activity was considerably lower than the one needed to replace the corresponding primer/template. This suggests that complete replacement of the primer/template is not required for the inhibition of DNA-dependent polymerase activity by SY-3E4. By contrast, the SY-3E4 concentrations required to inhibit RNA-dependent polymerase activity or replace primer/template were comparable in magnitude, which indicates that RNA-dependent polymerase activity is more difficult to inhibit by a small molecule.

The mechanism of interference with HIV-1 RT activity proposed here for SY-3E4 has not yet been explored for targeting, which is remarkable in light of a finding by Fisher and colleagues regarding the emergence of resistance to primer/template-competing inhibitors [24]. This study reported that mutations in HIV-1 RT that confer resistance to inhibitory aptamers [25] result in replication-defective HIV-1 by affecting primer/template interactions. The two mutants, N255D and N265D, map to the RT thumb domain and contact the primer/template. A subsequent study showed that these aptamer-resistant mutations retain their susceptibility to all NRTIs and NNRTIs tested in vitro [26]. In addition, the N265D mutation severely affected processivity of DNA-dependent DNA polymerase activity, but not that of RNA-dependent DNA polymerase activity. The N255D mutation affected the processivity of both activities severely [27]. Thus, the aptamer-resistant-conferring mutation N265D and compound SY-3E4 display a similar inhibitory profile. Considering the drug-resistant mutation-independent mechanism of SY-3E4 inhibition, it is possible that SY-3E4 treatment might also induce mutations in HIV-1 RT (like the aptamer) that could be suicidal or compromise enzymatic activity. Together with the recent finding that anti-RT aptamers are able to block HIV replication more potently than shRNAs [28–30], this would

open up conceptually novel avenues for the treatment of viral diseases.

SIGNIFICANCE

We have used an aptamer-displacement assay based on a highly modular and generally applicable protein-responsive ribozyme to identify a small-molecule antagonist for the human immunodeficiency virus type-1 reverse transcriptase (HIV-1 RT). Advancing beyond proof of principle, we show that this compound can inhibit the replication of HIV-1 wild-type and a multidrug-resistant strain. Thus, the compound's function is not affected by known drug-resistant mutations. An analysis of available crystallographic data of HIV-1 and HIV-2 RTs, complemented by characteristics of the inhibitory profile of the compound, identifies a region in these proteins as a previously unconsidered drugable interface that can be targeted by a small molecule. Since there are currently no small-molecule inhibitors available in the clinic that target this new site, our findings represent a major advance in the systematic exploration of alternative target sites in enzymes of viral and other pathogens with small molecules.

EXPERIMENTAL PROCEDURES

Small-Molecule Library
We used a commercially compiled library of 2500 structurally diverse "drug-like" compounds of many different compound classes (ComGenex, Hungary) that adhered to Lipinski's "rule-of-five" [31]. Each compound had a molecular weight below 550 Da.

Reporter Ribozyme Screening Assay
The screening assay was performed in 384-well plates. Each reaction was carried out in total volume of 25 μl under multiple turnover conditions with excess FRET substrate (200 nM) over the reporter ribozyme FK-1 (10 nM) in HH buffer (50 mM Tris/HCl [pH 7.9], 25 mM NaCl) at 37°C in the presence of HIV-1 RT (200 nM) and a small-molecule entity (100 μM) from the library by using an automated liquid-handling system (Tecan) with ceramic tips. The enzyme mixture had to be prepared in Pyrex glass vials for robotic operation. After the plates were preincubated for 15 min at 37°C in an Ascent Fluoroskan apparatus, the ribozyme reaction was initiated by adding MgCl$_2$ to a final concentration of 8 mM. The cleavage reaction was monitored in real time by measuring FAM-dye fluorescent emission (520 nm) for 15 min at 60 s intervals at a fixed excitation wavelength (492 nm). Negative control without HIV-1 RT was included for each compound. Each plate also contained a standard ribozyme reaction without compound as a positive control. Reactions were done in duplicate. The initial velocity (fluorescence/min) was determined by plotting the increment of fluorescence intensity, multiplied by a factor of 10,000, versus time. For each compound, the relative ribozyme activity (A_{rel}) was calculated by using the equation $A_{rel} = V_{RT+}/V_{RT-}$ (A_{rel} = relative activity, V_{RT+} = average number of initial velocity of ribozyme in the presence of HIV-1 RT, V_{RT-} = average number of initial velocity of ribozyme in the absence of HIV-1 RT). The standard reaction without compound usually gave the A_{rel} value of 0.2–0.3 depending on the plate. The compounds that showed a value of $A_{rel} > 0.4$ were identified as hits and were selected for testing.

In Vitro Polymerase Inhibition Assay
The RNA-dependent DNA polymerase activity was assayed by monitoring the RNA template/DNA primer-directed incorporation of dNTPs,

while the DNA-dependent DNA polymerase activity was assayed by DNA template/DNA primer-directed incorporation of dNTPs. After heat denaturing at 95°C for 5 min (RNA template/DNA primer denaturing at 70°C), the DNA template (10 μM) was annealed to a 5'-^{32}P-end labeled complementary DNA primer (3 μM) by slow cooling to room temperature for 1 hr. The small-molecule inhibitors were preincubated at 37°C for 5 min at various concentrations in the enzyme mixture containing 14 nM HIV-1 RT and 50 μM dNTP. Polymerase reactions were carried out in 20 μl volumes, containing 50 mM Tris/HCl (pH 8.0), 50 mM KCl, and 10 mM MgCl$_2$. The reactions were initiated by the addition of DNA template/5'-[^{32}P]-DNA primer complex and incubated at 37°C for 15 min. The polymerase activity was deactivated by the addition of 40 μl STOP solution (80% formamide, 20 mM EDTA) and denatured by heating at 95°C for 5 min prior to gel analysis (15% sequencing gel). The gel was visualized by autoradiography, and the amount of DNA synthesized was quantified by phosphor imaging analysis. IC$_{50}$ values were calculated from the inhibition dose-dependent curves by using Origin software. Assays of HIV-2 RT, AMV, MMLV, Klenow fragment, and human DNA polymerase β were carried out in the buffers supplied by the manufacturers. The reaction time was elongated to 1 hr for the Klenow fragment and human DNA polymerase β. Optionally, the concentration of dNTP was increased to 200 μM.

HIV-1 Replication Assay
A total of 2 $\times$ 10^4 TZM cells were grown in a 48-well plate. Different concentrations of compounds dissolved in 2 μl 100% DMSO were diluted in 150 μl cell culture medium (DMEM), then 50 μl virus containing solution (= 10,000 infectious units; infectivity was determined as tissue culture infectious dose 50% [TCID50] on C8166 cells) was added to a final concentration of 1% DMSO. TZM cells were infected with 200 μl DMEM containing virus and inhibitor after removal of old medium. After incubation for 2 days at 37°C under 5% CO$_2$ atmosphere, the luciferase marker gene expression, under the control of the HIV-1 LTR promoter, was measured (Steady-Glo luciferase assay, Promega). NL4-3 that had been produced in a coculture with C8166 cells was used as virus.

Infectivity Assay
Fresh coculture was prepared by dilution of coculture of NL4-3 virus with uninfected MT4 cells in the ratio of 1:10 (1 $\times$ 10^6 MT4/ml). After 4 hr of incubation at 37°C under 5% CO$_2$ atmosphere, 500 μl coculture and 5 μl different concentrations of inhibitors were added to each 48 well. After 2 days at 37°C under 5% CO$_2$, cell-free supernatant of the MT4 coculture was used to infect TZM cells, which enables the determination of the amount of infectious particles that have been produced in the presence of inhibitor. A total of 2 days postinfection, cells were fixed with 3% PFA for 30 min and were washed with PBS. The infected TZM cells were stained with β-galactosidase substrate (TZM cells also contain a β-galactosidase reporter gene under the control of HIV-1 LTR). After 2–3 hr of incubation at 37°C, infected cells turned blue and were counted under the microscope.

Residue Mapping and Structure Analysis
Structural and mutant data analyzed herein are summarized in Table S1. For structure analysis and comparison, residue mapping, and the generation of graphical representations, the Molecular Operating Environment (MOE, Chemical Computing Group, Inc.; http://www.chemcomp.com) was used.

Supplemental Data
Supplemental data include four figures and a table and can be found with this article online at http://www.chembiol.com/cgi/content/full/14/7/804/DC1/.

REFERENCES

1. Dobson, C.M. (2004). Chemical space and biology. Nature *432*, 824–828.

2. Bohacek, R.S., McMartin, C., and Guida, W.C. (1996). The art and practice of structure-based drug design: a molecular modeling perspective. Med. Res. Rev. *16*, 3–50.

3. Bradley, D. (2004). In need of more space. (http://www.nature.com/horizon/chemicalspace/background/synthesis.html).

4. Jenne, A., Hartig, J.S., Piganeau, N., Tauer, A., Samarsky, D.A., Green, M.R., Davies, J., and Famulok, M. (2001). Rapid identification and characterization of hammerhead-ribozyme inhibitors using fluorescence-based technology. Nat. Biotechnol. *19*, 56–61.

5. Hartig, J.S., Najafi-Shoushtari, S.H., Grune, I., Yan, A., Ellington, A.D., and Famulok, M. (2002). Protein-dependent ribozymes report molecular interactions in real time. Nat. Biotechnol. *20*, 717–722.

6. Hafner, M., Schmitz, A., Grune, I., Srivatsan, S.G., Paul, B., Kolanus, W., Quast, T., Kremmer, E., Bauer, I., and Famulok, M. (2006). Inhibition of cytohesins by SecinH3 leads to hepatic insulin resistance. Nature *444*, 941–944.

7. Hartig, J.S., and Famulok, M. (2002). Reporter ribozymes for real-time analysis of domain-specific interactions in biomolecules: HIV-1 reverse transcriptase and the primer-template complex. Angew. Chem. Int. Ed. *41*, 4263–4266.

8. Tuerk, C., MacDougal, S., and Gold, L. (1992). RNA pseudoknots that inhibit human immunodeficiency virus type 1 reverse transcriptase. Proc. Natl. Acad. Sci. USA *89*, 6988–6992.

9. Soukup, G.A., and Breaker, R.R. (1999). Nucleic acid molecular switches. Trends Biotechnol. *17*, 469–476.

10. Famulok, M. (1999). Oligonucleotide aptamers that recognize small molecules. Curr. Opin. Struct. Biol. *9*, 324–329.

11. Breaker, R.R. (2002). Engineered allosteric ribozymes as biosensor components. Curr. Opin. Biotechnol. *13*, 31–39.

12. Silverman, S.K. (2003). Rube Goldberg goes (ribo)nuclear? Molecular switches and sensors made from RNA. RNA *9*, 377–383.

13. Famulok, M. (2005). Allosteric aptamers and aptazymes as probes for screening approaches. Curr. Opin. Mol. Ther. *7*, 137–143.

14. Jarmy, G., Heinkelein, M., Weissbrich, B., Jassoy, C., and Rethwilm, A. (2001). Phenotypic analysis of the sensitivity of HIV-1 to inhibitors of the reverse transcriptase, protease, and integrase using a self-inactivating virus vector system. J. Med. Virol. *64*, 223–231.

15. Wei, X., Decker, J.M., Liu, H., Zhang, Z., Arani, R.B., Kilby, J.M., Saag, M.S., Wu, X., Shaw, G.M., and Kappes, J.C. (2002). Emergence of resistant human immunodeficiency virus type 1 in patients receiving fusion inhibitor (T-20) monotherapy. Antimicrob. Agents Chemother. *46*, 1896–1905.

16. Summerer, D., and Marx, A. (2001). DNA polymerase selectivity: sugar interactions monitored with high-fidelity nucleotides. Angew. Chem. Int. Ed. *40*, 3693–3695.

17. Sarafianos, S.G., Das, K., Tantillo, C., Clark, A.D., Jr., Ding, J., Whitcomb, J.M., Boyer, P.L., Hughes, S.H., and Arnold, E. (2001). Crystal structure of HIV-1 reverse transcriptase in complex with a polypurine tract RNA:DNA. EMBO J. *20*, 1449–1461.

18. Ren, J., Esnouf, R., Garman, E., Somers, D., Ross, C., Kirby, I., Keeling, J., Darby, G., Jones, Y., Stuart, D., et al. (1995). High resolution structures of HIV-1 RT from four RT-inhibitor complexes. Nat. Struct. Biol. *2*, 293–302.

19. Huang, H., Chopra, R., Verdine, G.L., and Harrison, S.C. (1998). Structure of a covalently trapped catalytic complex of HIV-1 reverse transcriptase: implications for drug resistance. Science *282*, 1669–1675.

20. Jaeger, J., Restle, T., and Steitz, T.A. (1998). The structure of HIV-1 reverse transcriptase complexed with an RNA pseudoknot inhibitor. EMBO J. *17*, 4535–4542.

21. Shafer, R.W., Rhee, S.-Y., Kiuchi, M., Liu, T., Zioni, R., Gifford, R.J., Wang, C., Khan, Z., Goldman, S., Mitsuya, Y., et al. (2006). Stanford University HIV Drug Resistance Database (http://hivdb.stanford.edu/).

22. Kensch, O., Connolly, B.A., Steinhoff, H.J., McGregor, A., Goody, R.S., and Restle, T. (2000). HIV-1 reverse transcriptase-pseudoknot RNA aptamer interaction has a binding affinity in the low picomolar range coupled with high specificity. J. Biol. Chem. *275*, 18271–18278.

23. Ren, J., Bird, L.E., Chamberlain, P.P., Stewart-Jones, G.B., Stuart, D.I., and Stammers, D.K. (2002). Structure of HIV-2 reverse transcriptase at 2.35-Å resolution and the mechanism of resistance to non-nucleoside inhibitors. Proc. Natl. Acad. Sci. USA *99*, 14410–14415.

24. Fisher, T.S., Joshi, P., and Prasad, V.R. (2002). Mutations that confer resistance to template-analog inhibitors of human immunodeficiency virus (HIV) type 1 reverse transcriptase lead to severe defects in HIV replication. J. Virol. *76*, 4068–4072.

25. Schneider, D.J., Feigon, J., Hostomsky, Z., and Gold, L. (1995). High-affinity ssDNA inhibitors of the reverse transcriptase of type 1 human immunodeficiency virus. Biochemistry *34*, 9599–9610.

26. Fisher, T.S., Joshi, P., and Prasad, V.R. (2005). HIV-1 reverse transcriptase mutations that confer decreased in vitro susceptibility to anti-RT DNA aptamer RT1t49 confer cross resistance to other anti-RT aptamers but not to standard RT inhibitors. AIDS Res. Ther. *2*, 8.

27. Fisher, T.S., Darden, T., and Prasad, V.R. (2003). Mutations proximal to the minor groove-binding track of human immunodeficiency virus type 1 reverse transcriptase differentially affect utilization of RNA versus DNA as template. J. Virol. *77*, 5837–5845.

28. Joshi, P., and Prasad, V.R. (2002). Potent inhibition of human immunodeficiency virus type 1 replication by template analog reverse transcriptase inhibitors derived by SELEX (systematic evolution of ligands by exponential enrichment). J. Virol. *76*, 6545–6557.

29. Joshi, P.J., North, T.W., and Prasad, V.R. (2005). Aptamers directed to HIV-1 reverse transcriptase display greater efficacy over small hairpin RNAs targeted to viral RNA in blocking HIV-1 replication. Mol. Ther. *11*, 677–686.

30. Held, D.M., Kissel, J.D., Thacker, S.J., Michalowski, D., Saran, D., Ji, J., Hardy, R.W., Rossi, J.J., and Burke, D.H. (2007). Cross-clade inhibition of recombinant human immunodeficiency virus type 1 (HIV-1), HIV-2, and simian immunodeficiency virus SIVcpz reverse transcriptases by RNA pseudoknot aptamers. J. Virol. *81*, 5375–5384.

31. Lipinski, C.A., Lombardo, F., Dominy, B.W., and Feeney, P.J. (2001). Experimental and computational approaches to estimate solubility and permeability in drug discovery and development settings. Adv. Drug Deliv. Rev. *46*, 3–26.